

THE NATURE OF Mn-Mn COUPLING IN Mn-Ni-Al ALLOYS

V. REDNIC^{1*}, M. COLDEA², V. POP², M. NEUMANN³

ABSTRACT. The occurrence of ferro - and antiferromagnetism in Mn-Ni-Al alloys is governed by the sign of the direct exchange interaction between the Mn magnetic ions. Experimentally has been found that, if the separation between the Mn magnetic ions is greater than the critical value $d_{cr} = 2.91 \text{ \AA}$, they are ferromagnetic and if the distance is less than the critical value, they are antiferromagnetic. The value of Mn local magnetic moment depends on the number of Al atoms in the first vicinity but the dominant factor is the Mn-Al distance. The nature of Mn-Mn exchange coupling was studied through X-ray diffraction, magnetic and XPS measurements.

Keywords: *exchange coupling, local magnetic moments, crystallographic structure, electronic structure*

INTRODUCTION

The problem of local moments confined to the transition 3d metals (T) sites, i.e., localized behaviour in some aspects of itinerant electrons, is one of the most important issues in the physics of the magnetic alloys and intermetallic compounds [1]. The condition for the existence of the local moment at the T site is $\pi\Delta / U < 1$, where Δ is the width of the d states and U is the Coulomb correlation energy between d electrons [2]. The occurrence of ferro and antiferromagnetism in alloys and intermetallic compounds of 3d metals Mn, Cr, Fe is governed by the sign of the direct exchange interaction between the magnetic ions. Experimentally has been found that, in general, if the separation between the magnetic ions is greater than a critical value d_{cr} , they are ferromagnetic and if the distance is less

¹ National Institute for Research and Development of Isotopic and Molecular Technologies, P.O. Box 700, 400293 Cluj-Napoca, Romania

² Babes-Bolyai University, Faculty of Physics, Kogalniceanu 1, 400084 Cluj-Napoca, Romania

³ University of Osnabrück, Fachbereich Physik, 49069 Osnabrück, Germany

* Corresponding author: vasile.rednic@itim-cj.ro

than the critical value, they are antiferromagnetic. In general, the Mn alloys and intermetallic compounds are antiferromagnetic when the distance between the Mn atoms $d_{\text{Mn-Mn}}$ is less than 2.9 Å [3]. Experimentally, the critical Mn-Mn distance of 2.83 Å has been estimated in NiAs-type Mn compounds [3,4]. On the other hand, the magnetic τ -phase of MnAl alloy shows ferromagnetism at a high Curie temperature despite the very short Mn-Mn distance of 2.77 Å [5]. This, the so-called Mn dilemma, is based on the simple Bethe-Slater picture of direct exchange coupling between magnetic atoms [6, 7]. It was found that super-exchange interaction between Mn atoms via p-electrons of Al atoms causes antiferromagnetism in MnAl τ -phase. The ferromagnetism in this system results from the suppression of the super-exchange interaction due to the substitution of excess Mn atoms for the Al atoms, so the Mn-Mn distance does not strongly affect the magnetism in this alloy [5].

In the phase diagram of Mn-Ni-Al ternary system there are many domains of solid solution [8]. Maintaining constant the concentration of one element, one can vary the concentration of the other two elements. In this case are changing the crystalline structure, the number of near- neighbours atoms with d-orbitals, the vicinity of Mn atoms, the distances between the Mn atoms and implicitly the strength and the sign of the interaction between the neighbouring local moments.

The aim of this paper is to study, through X-ray diffraction, magnetic and XPS measurements, the nature of Mn-Mn exchange in the Mn-Ni-Al alloys.

EXPERIMENTAL

The investigated alloys were prepared by the argon arc melting method. The samples were melted repeatedly (at least four times) in the same atmosphere to ensure homogeneity. The weight loss of the final furnace-cooled samples was found to be less than 1%. The purity of starting materials was 99.999% for Al and 99.99% for Mn and Ni. XRD measurements were performed on polished surfaces using a Bruker D8 Advance diffractometer, due to the hardness of the samples. The magnetic measurements were performed using a vibrating sample magnetometer (VSM) in the temperature range 4– 850 K and fields up to 10 T. The XPS spectra were recorded using a PHI 5600ci ESCA spectrometer with monochromatized Al K α radiation at room temperature. The pressure in the ultra-high vacuum chamber was in the 10⁻¹⁰ mbar range during the measurements. The samples were cleaved in situ and the surface cleanness was checked by monitoring the O 1s and C 1s core levels in the survey spectra.

RESULTS AND DISCUSSIONS

The nature of Mn-Mn exchange coupling is described by two main characteristics namely, the sign and the strength of the exchange coupling. The sign of the exchange coupling is mostly given by the Mn-Mn distance, while the strength depends on the number and type of the surrounding atoms as well as the distance between them.

The sign of Mn-Mn exchange coupling

One of the most representative system where the influence of Mn-Mn critical distance can be observed is $\text{Ni}_{1-x}\text{Mn}_x\text{Al}$. The electronic structure and magnetic properties of $\text{Ni}_{1-x}\text{Mn}_x\text{Al}$ ($x=0, 0.2, 0.3, 0.4, 0.5, 0.6, 0.8$) were presented [9]. X-ray diffraction patterns show that all the alloys are single phases with the same CsCl (B2) structure type. In the elementary cell Al atoms occupies the 1a position while Mn and Ni atoms occupy the 1b position (see figure 1). When two Mn atoms are situated in the centre of two neighbouring elementary cells, the shorter Mn-Mn distance is equal to the lattice parameter. In this system the lattice parameter is close to the critical Mn-Mn distance (~ 2.9 Å). Furthermore, the lattice parameter (see figure 1) increases monotonically with Mn concentration from $a=2.875$ Å for NiAl to $a=2.966$ Å for $\text{Ni}_{0.2}\text{Mn}_{0.8}\text{Al}$.

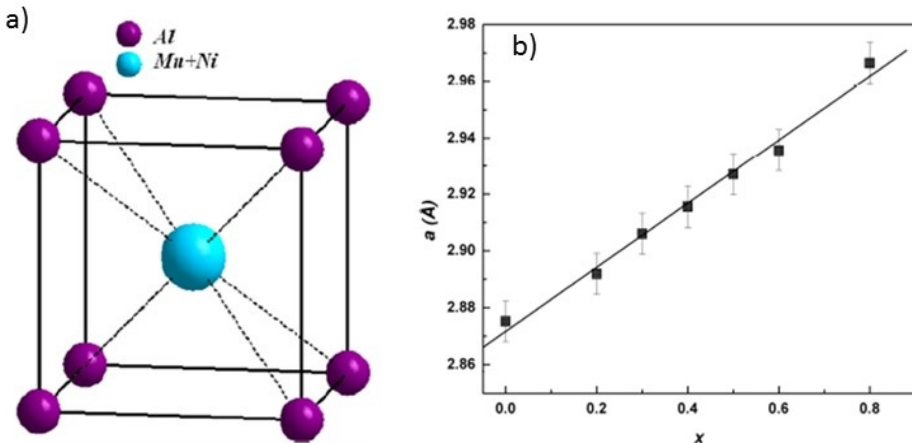


Fig. 1. Elementary cell representation (a) and lattice parameter variation as a function of Mn content (b) in $\text{Ni}_{1-x}\text{Mn}_x\text{Al}$ alloys.

The temperature dependence of the spontaneous magnetization, presented in figure 2, shows a ferromagnetic behaviour of the investigated alloys. Nevertheless, a small anomaly in the magnetization of the ferromagnetic component can be observed at low Mn concentration ($x = 0.2$ and 0.3). This anomaly, known as “pinning effect”, comes from the exchange interaction at the interfaces of an antiferromagnetic and a ferromagnetic entity, and proves the formation of Mn-Mn antiferromagnetic pairs.

At low Mn concentration the lattice parameter is smaller than the critical distance favouring the formation of Mn-Mn antiferromagnetic pairs, but in the same time, at small Mn concentration there is a smaller probability to have two Mn atoms in the centre of two neighbouring cells. This explains the ferromagnetic behaviour of these alloys and also the presence of a small antiferromagnetic phase.

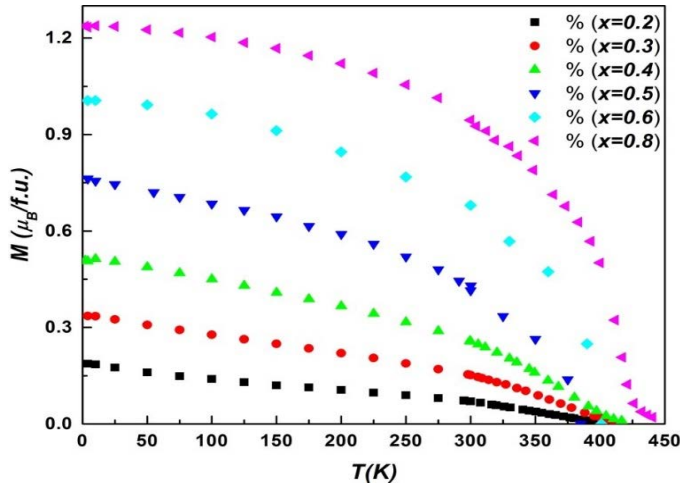


Fig. 2. Temperature dependence of spontaneous magnetization of $\text{Ni}_{1-x}\text{Mn}_x\text{Al}$ alloys. [9]

Once the Mn concentration increases, the probability of having two Mn atoms in the centre of two neighbour cell increases, suggesting an increase in the number of antiferromagnetic Mn-Mn pairs. The experimental results show that the antiferromagnetic component is barely visible for $x=0.4$ and disappears for higher Mn concentration. This can be explained by the increase of the lattice parameter, and consequently the Mn-Mn distance, at values above 2.9 \AA . This means that even if there are two Mn atoms in centre of two neighbour cells, the distance between them is higher than the critical distance and consequently the exchange coupling is ferromagnetic.

The “pinning” effect was also observed in **$\text{Mn}_{1-x}\text{Al}_x\text{Ni}$ alloys** [10], where a coexistence of antiferromagnetism (B2 phase) and ferromagnetism ($L2_1$ phase) was observed for $0.6 \leq x < 1$ alloys. The B2 phase has the same structure with the $L2_1$

phase of Heusler alloys, having the unit cell equals with the 8-th part from the last one (see figure 3). In the L2₁ structure, where the Mn atoms are separated by Al atoms, the shortest Mn-Mn distance is about 4.1Å, while in B2 phase the Mn and Al atoms are randomly arranged, thus the near-neighbour Mn-Mn distance is about 2.9 Å.

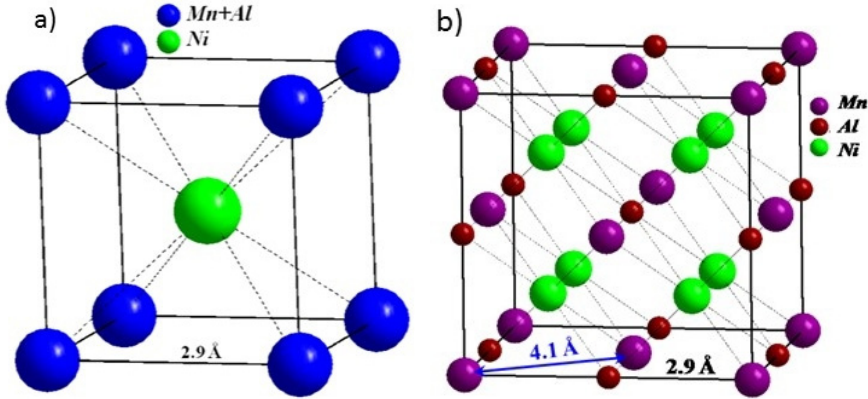


Fig. 3. Representation of ClCs (a) and Heusler (b) structure type.

In order to determine the ferromagnetic (FM) and antiferromagnetic (AFM) contributions to the measured magnetization and to estimate the corresponding Curie and Néel temperatures T_C and respectively T_N , we have used the Honda-Arrot plot for each temperature, according to the relation [11]:

$$\chi_m = \chi_{AFM} + M_{FM}/H \quad (1)$$

where χ_m is the measured susceptibility, χ_{AFM} the susceptibility of the antiferromagnetic component, M_{FM} the saturation magnetization of the ferromagnetic component and H the applied magnetic field. A linear dependence of χ_m versus H^{-1} in higher magnetic fields was evidenced for each temperature, showing that in the studied field range, saturation has been obtained. In figure 4 are shown the temperature dependence of the as determined susceptibility χ_{AFM} and magnetization M_{FM} , respectively. The curves $\chi_{AFM}(T)$ present a downward at certain temperatures, referred as the Néel temperatures.

The Mn-Mn exchange coupling depending on Mn-Mn distance was also evidenced in **Ni_{0.7-x}Al_xMn_{0.3}** alloys. The crystallographic and electronic structure of Ni_{0.7-x}Al_xMn_{0.3} alloys were presented [12]. The Ni_{0.7-x}Al_xMn_{0.3} ($x=0.3, 0.4$ and 0.5) alloys are single phase having CsCl (B2) structure type. The lattice parameter varies from 2.9 Å for $x=0.3$ to 2.94 Å for $x=0.5$. The lattice parameter and implicit the Mn-Mn atomic distance is just in the region of Mn-Mn critical distance and the effect on magnetic properties are significant as it can be seen in figure 5.

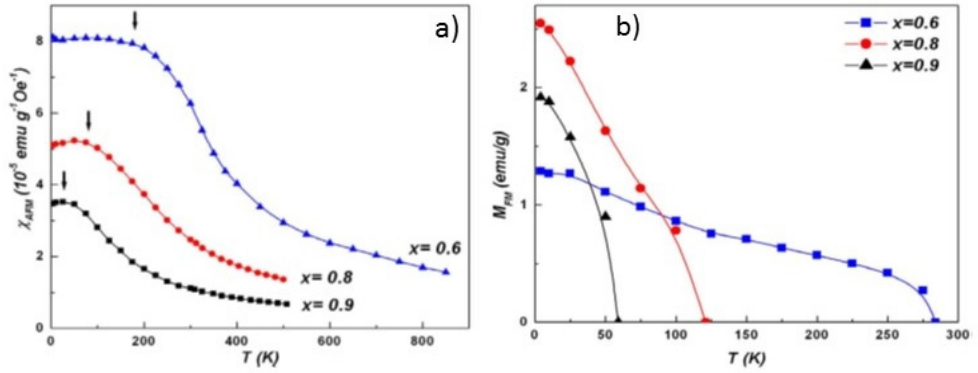


Fig. 4. The temperature dependence of the magnetic susceptibility χ_{AFM} (a) and the magnetization (b) of $\text{Mn}_{1-x}\text{Al}_x\text{Ni}$ alloys. The arrows indicate the Néel temperatures. [10].

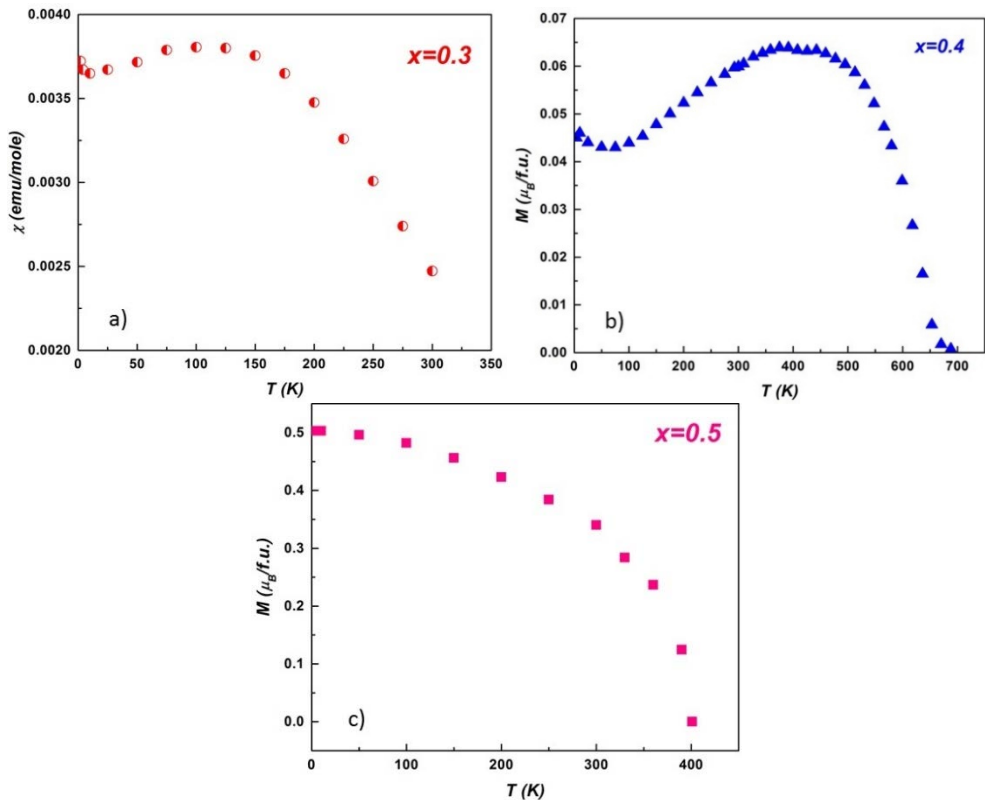


Fig. 5. The temperature dependence of magnetic susceptibility (a) and the spontaneous magnetization (b and c) of $\text{Ni}_{0.7-x}\text{Al}_x\text{Mn}_{0.3}$ alloys.

The $\text{Ni}_{0.4}\text{Al}_{0.3}\text{Mn}_{0.3}$ alloy has the lattice parameter $a \approx 2.90 \text{ \AA}$. At this distance the Mn-Mn coupling is antiferromagnetic. The $\text{Ni}_{0.3}\text{Al}_{0.4}\text{Mn}_{0.3}$ alloy has the lattice parameter a little bit larger $a \approx 2.914 \text{ \AA}$, but seems to be at the limit distance between the AFM and FM coupling. This could be a reason why this alloy has ferrimagnetic behaviour. The lattice parameter of the $\text{Ni}_{0.2}\text{Al}_{0.5}\text{Mn}_{0.3}$ alloy is larger ($a \approx 2.94 \text{ \AA}$) and it has a ferromagnetic behaviour. This means that at this distance the coupling between the Mn atoms is parallel.

The strength of Mn-Mn interaction

The strength of Mn-Mn interaction and consequently the value of Mn local magnetic moments strongly depend on surrounding atoms. The Mn magnetic moment is sensitive to the type, the number and the distance to the atoms from the first coordination shell. These factors will influence the hybridization degree of Mn 3d band. In Mn-Ni-Al system, the Al atoms bring 3 valence electrons. The hybridization between Mn 3d state and Al 3sp states leads to a partial filling of Mn 3d band and consequently a reduction on Mn magnetic moment (the higher the hybridization degree the lower Mn magnetic moment will be). The hybridization degree depends on the number of Al atoms from Mn first coordination shell and Mn-Al distance. To support these affirmations we analysed the influence of Mn 3d - Al 3sp hybridization on Mn magnetic moment in two systems: a) $\text{Mn}_{1-x}\text{Al}_x\text{Ni}$ (0 - 8 Al atoms in the first vicinity of Mn atoms, at $d_{\text{Mn-Al}} \approx 2.9 \text{ \AA}$) and b) $\text{Ni}_{1-x}\text{Mn}_x\text{Al}$ (8 Al atoms in the first vicinity of Mn atoms, at $d_{\text{Mn-Al}} \approx 2.5 \text{ \AA}$). XPS measurements correlated with magnetic measurements are further presented for both cases.

a) The Mn 3s spectra for MnNi, $\text{Mn}_{0.9}\text{Al}_{0.1}\text{Ni}$ and $\text{Mn}_{0.8}\text{Al}_{0.2}\text{Ni}$ are shown in figure 6. The shoulder around 79 eV corresponds to the Ni 3p satellite situated at about 12 eV higher binding energy from the main line [13].

The experimental spectra were fitted with two components corresponding to Mn 3s exchange splitting, the Ni 3p satellite and a Shirley background type. Figure 6b presents the curve fitting results of MnNi compound, after background and Ni 3p satellite subtraction. Similar results were obtained for the other two alloys $\text{Mn}_{0.9}\text{Al}_{0.1}\text{Ni}$ and $\text{Mn}_{0.8}\text{Al}_{0.2}\text{Ni}$. All spectra exhibit a well-defined magnetic exchange splitting of about 5 eV, arising from the exchange interactions between the 3s core hole and open Mn 3d shell. This splitting corresponds to a spin $S \approx 2$ and a magnetic moment of $4 \mu_B/\text{Mn}$, suggesting that at this Mn-Al distance (2.9 Å) the Mn 3d band is not affected by the hybridization with Al 3sp states. Magnetic measurements confirm just a small variation of Mn magnetic moments, once the Al concentration increases, compared to MnNi compound [10].

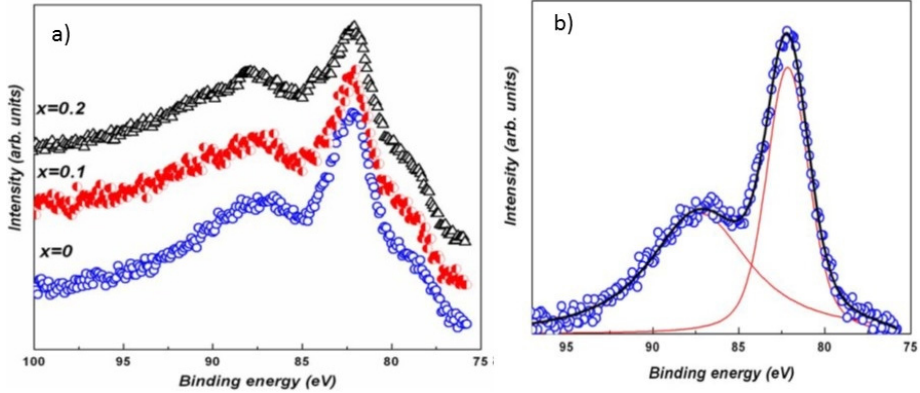


Fig. 6. Mn 3s XPS spectra of $Mn_{1-x}Al_xNi$ alloys (a) and Mn 3s curve fitting results of MnNi compound (b). [10]

b). In the second system $Ni_{1-x}Mn_xAl$, the Mn 3s core level spectra show an exchange splitting of around 4 eV, which is smaller compared to the exchange splitting in $Mn_{1-x}Al_xNi$ alloys (5.2 eV). The exchange splitting is proportional with the Mn local magnetic moment [13]. Figure 7 presents the curve fitting results of $Mn_{0.8}Ni_{0.2}Al$ alloy, after background subtraction, and the similar spectrum of MnNi compound for comparison.

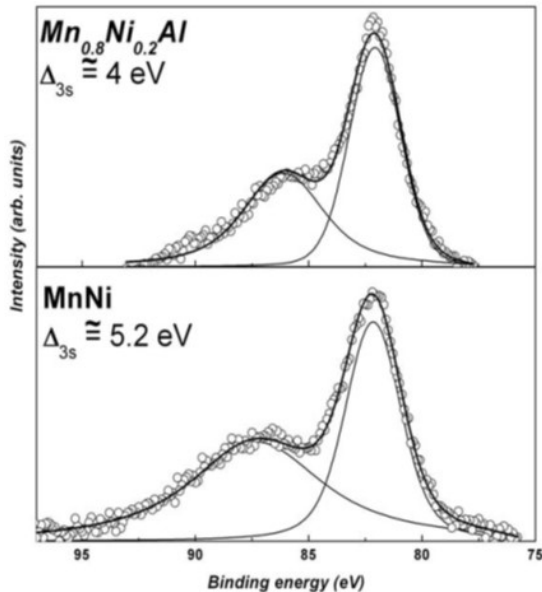


Fig. 7. Mn 3s curve fitting results of $Mn_{0.8}Ni_{0.2}Al$ alloy and MnNi compound. [9]

The strong Mn 3d - Al 3sp hybridization is due to the high number of Al atoms in the Mn first vicinity, namely 8 Al atoms at ~ 2.5 Å. This explains the small values of the Mn magnetic moments (below $2\mu_B$) in $\text{Ni}_{1-x}\text{Mn}_x\text{Al}$ alloys [9] comparing to $\text{Mn}_{1-x}\text{Al}_x\text{Ni}$ alloys.

The Mn magnetic moment slowly increases with Mn concentration [9]. This variation can be associated with the increase of the lattice parameter which leads to a decreasing in the Mn 3d - Al 3sp hybridization degree.

CONCLUSIONS

We evidence a value of about 2.91 Å as the critical Mn-Mn distance in Mn-Ni-Al alloys. Experimentally we demonstrated that, if the separation between the Mn atoms is greater than this critical value, the exchange coupling is ferromagnetic and if the distance is smaller than the critical value, the exchange coupling is antiferromagnetic. The value of Mn local magnetic moment depends on the number of Al atoms in the first vicinity but the dominant factor is the Mn-Al distance. When the Mn-Al distance is about 2.9 Å the Mn 3d band is not affected by the hybridization but, at lower Mn-Al distance (~ 2.5 Å) the hybridization between Mn 3d and Al 3sp states leads to a partial filling of Mn 3d band and a drastically reduction of Mn local magnetic moment.

REFERENCES

- [1] V. Yu. Irkhin, M. I. Katsnelson, A. V. Trefilov, *J. Phys.: Cond. Matter.*, 5, 8763 (1993).
- [2] P.W.Anderson, *Phys. Rev.*, 124, 41-53 (1961).
- [3] V. Seshu Bai, T. Rajasekharan, *J. Magn. Magn. Mat.*, 42, 198-200 (1984).
- [4] R. Forrer, *Ann.de Phys.*, 7, 605 (1952).
- [5] Suguru Sato, Shuichiro Irie, Yuki Nagamine, Tasashi Miyazaki, Yuji Umeda, *Scientific reports*, <https://doi.org/10.1038/s41598-020-69538-2>
- [6] J. C. Slater, *Phys. Rev.*, 36, 57 (1930).
- [7] H. Bethe, „Handbook of Physics”, Vol 24/2 (Springer-Verlag, Berlin, 1933) p. 595.
- [8] V. Raghavan, *Journal of Phase Equilibria and Diffusion*, 27 (5), 493-496 (2006).
- [9] V. Rednic, O. Isnard, M. Neumann, L. Rednic, M. Coldea, N. Aldea, *J. Optoelectron. Adv. Mat.*, 13(11-12), 1519-1523 (2011).
- [10] V. Rednic, M. Coldea, S. K. Mendiratta, M. Valente, V. Pop, M. Neumann and L. Rednic, *J. Mag. Mag. Mat.*, 321, 3415–3421 (2009).
- [11] L. F. Bates, “Modern Magnetism”, Cambridge Univ. Press, Cambridge, 1951.

- [12] V. Rednic, M. Coldea, O. Isnard, M. Neumann and L. Rednic, *Studia Universitatis Babeş-Bolyai Physica*, LIV (1), 79-85 (2009).
- [13] S. Hüfner, "Photoelectron Spectroscopy Principles and Applications", Springer-Verlag, Berlin (1995), p. 89.